Am J Physiol Heart Circ Physiol 300: H459–H467, 2011.
First published November 12, 2010; doi:10.1152/ajpheart.00244.2010.

Sprouty2 downregulates angiogenesis during mouse skin wound healing

Mateusz S. Wietecha,[1]* Lin Chen,[1]* Matthew J. Ranzer,[1] Kimberly Anderson,[2] Chunyi Ying,[2] Tarun B. Patel,[2] and Luisa A. DiPietro[1]

[1]*Center for Wound Healing and Tissue Regeneration, College of Dentistry, University of Illinois at Chicago, Chicago, and* [2]*Department of Molecular Pharmacology and Therapeutics, Stritch School of Medicine, Loyola University Medical Center, Maywood, Illinois*

Submitted 9 March 2010; accepted in final form 11 November 2010

Wietecha MS, Chen L, Ranzer MJ, Anderson K, Ying C, Patel TB, DiPietro LA. Sprouty2 downregulates angiogenesis during mouse skin wound healing. *Am J Physiol Heart Circ Physiol* 300: H459–H467, 2011. First published November 12, 2010; doi:10.1152/ajpheart.00244.2010.—Angiogenesis is regulated by signals received by receptor tyrosine kinases such as vascular endothelial growth factor receptors. Mammalian Sprouty (Spry) proteins are known to function by specifically antagonizing the activation of the mitogen-activated protein kinase signaling pathway by receptor tyrosine kinases, a pathway known to promote angiogenesis. To examine the role of Spry2 in the regulation of angiogenesis during wound repair, we used a model of murine dermal wound healing. Full-thickness excisional wounds (3 mm) were made on the dorsum of anesthetized adult female FVB mice. Samples were harvested at multiple time points postwounding and analyzed using real-time RT-PCR, Western blot analysis, and immunofluorescent histochemistry. Spry2 mRNA and protein levels in the wound bed increased significantly during the resolving phases of healing, coincident with the onset of vascular regression in this wound model. In another experiment, intracellular levels of Spry2 or its dominant-negative mutant (Y55F) were elevated by a topical application to the wounds of controlled-release gel containing cell permeable, transactivator of transcription-tagged Spry2, Spry2^{Y55F}, or green fluorescent protein (as control). Wound samples were analyzed for vascularity using CD31 immunofluorescent histochemistry as well as for total and phospho-Erk1/2 protein content. The treatment of wounds with Spry2 resulted in a significant decrease in vascularity and a reduced abundance of phospho-Erk1/2 compared with wounds treated with the green fluorescent protein control. In contrast, the wounds treated with the dominant-negative Spry2^{Y55F} exhibited a moderate increase in vascularity and elevated phospho-Erk1/2 content. These results indicate that endogenous Spry2 functions to downregulate angiogenesis in the healing murine skin wound, potentially by inhibiting the mitogen-activated protein kinase signaling pathway.

blood vessel; vascular regression; mitogen-activated protein kinase signaling; endothelial cell

ANGIOGENESIS, OR THE GROWTH of new blood vessels by way of sprouting from the preexisting vasculature, is a tightly regulated and complex biological process involving endothelial cell (EC) and vascular smooth muscle cell (VSMC) proliferation, differentiation, migration, and organization into a branched tubular network (14, 37). The reestablishment of a viable vascular network following trauma is one of the most important components of successful wound repair subsequent to hemostasis and inflammation (14). In the healing wound, robust angiogenesis is induced following the endogenous production and release of high amounts of proangiogenic agents, including platelet-derived growth factor (PDGF), fibroblast growth factor-2 (FGF-2), and vascular endothelial growth factor (VEGF) (14, 32, 33). These growth factors, via the downstream upregulation and amplification of signaling proteins in the Raf/Mek/Erk pathway in ECs and VSMCs, promote the dramatic cellular changes required for angiogenesis (37).

During the proangiogenic phase of dermal healing, vessel density in the wound more than doubles compared with vascularity levels observed in normal, uninjured skin (40). The regression of this newly formed vasculature is a critical component of the resolving dermal wound. After reaching a maximum vessel density, blood vessels in the wound are pruned back to levels observed in normal tissue until vascular homeostasis is achieved (40). Whereas the mechanisms that drive blood vessel formation in physiological and pathological wound models have been the topic of much investigation, the inhibition of angiogenesis followed by vascular regression in the context of wound healing has not been well studied and is thus not well understood.

Sprouty is an intracellular protein that includes four mammalian homologs (Spry1–4) which are expressed in most fetal and adult tissues during and after development (31). Besides their specific documented roles in the proper development of the murine hearing apparatus (39) and enteric neural network (42), Spry proteins are also ubiquitously produced in ECs and VSMCs (2), suggesting a widespread and varied physiological function spanning multiple cell types. In general, mammalian Spry proteins are negative feedback loop modulators of the Raf/Mek/Erk-associated signaling pathways downstream of major growth factor stimuli such as FGF, VEGF, and PDGF and have been found to regulate tubular morphogenesis (10, 16, 22, 34). Upon activation by growth factor binding to its compatible receptor tyrosine kinase (RTK), Spry is induced to translocate to the inner plasma membrane (16, 24, 27) where it interacts with various early mitogen-activated protein kinase (MAPK) pathway-associated proteins in a cell- and context-specific manner (10, 16, 22).

Early in vitro studies showed that Spry inhibits FGF- and VEGF-induced EC proliferation and differentiation via the downregulation of the Raf/Mek/Erk signaling pathway (24). Spry is upregulated concurrently with FGF downregulation during EC morphogenesis in three-dimensional collagen matrixes (6). Additionally, Spry2 has been shown to inhibit VSMC proliferation and migration (46). Lee et al. (26) demonstrated that an overexpression of Spry4 inhibited EC proliferation, migration, and MAPK activation in vitro as well as the branching and sprouting of blood vessels in murine embryos.

* M. S. Wietecha and L. Chen contributed equally to this study.

Address for reprint requests and other correspondence: L. A. DiPietro, Univ. of Illinois at Chicago, College of Dentistry, Center for Wound Healing & Tissue Regeneration (MC 859), 801 S. Paulina, Rm. 401B, Chicago, IL, 60612-7211 (e-mail: Ldipiet@uic.edu).

Recently, Taniguchi et al. (43) showed via in vivo murine knockout and knockdown analyses that Spry2 and Spry4 are negative regulators of angiogenesis. Specifically, Spry4 knockout mice were more resistant to hindlimb ischemia with increased blood vessel density in both muscle and skin, and in vivo small hairpin RNA knockdown of Spry2/4 accelerated angiogenesis in the murine hindlimb ischemia model (43).

These previous studies suggest that Spry may be an important endogenous antiangiogenic agent in mammals. We hypothesized that Spry2 may be involved in downregulating angiogenesis during the post-proliferative stage of murine dermal wound repair leading to blood vessel regression. In this study, we show that Spry2 is produced in the wound bed during the later phases of healing, coincident with the onset of vascular regression in this wound model. Cell permeable, transactivator of transcription (TAT)-tagged Spry2 inhibits EC migration and MAPK signaling. Furthermore, we show that the topical application of exogenous, cell permeable Spry2 onto dermal murine wounds downregulates angiogenesis as well as MAPK signaling.

MATERIALS AND METHODS

Animals and Wound Models

FVB-strain 6–8-wk-old female mice (Jackson, Bar Harbor, ME) were anesthetized using an intraperitoneal injection of 100 mg/kg ketamine and 5 mg/kg xylazine solution, and their dorsal skin was shaved and cleansed with 70% isopropyl alcohol. Six excisional full-thickness dermal wounds were made on the dorsal surface of each mouse, three on both sides of the midline, using a sterile 3-mm punch-biopsy instrument (Acu Punch, Acuderm, Ft. Lauderdale, FL). Standard aseptic techniques were followed. The excised skin was used as normal, unwounded skin control. At 1, 3, 5, 7, 10, 14, 21, and 28 days after injury, five mice per time point were euthanized and the wounds harvested. Two samples per mouse were placed in RNAlater (Sigma, St. Louis, MO) solution for real-time RT-PCR analysis, two were snap frozen for protein analysis, and two were placed in optimum cutting temperature (OCT) compound (Sakura Finetechnical, Tokyo, Japan) and snap frozen for cryosectioning and immunofluorescent histochemistry. To control for the contraction of murine excisional wounds, 5-mm punch-biopsy instruments were used for the collection of wound samples until the *day 5* time point, and 3-mm punch-biopsy instruments were used for wound harvesting during later time points; thus, all harvested wound samples from the various time points ended up with approximately the same amount of surrounding unwounded tissue relative to the wound area. The underside of the skin with its unique postwounding revascularization pattern as well as the presence of a scar (characterized by the lack of hair) are two methods that were used for the identification of the wound area during later time points, especially on *days 21* and *28* postwounding.

The mice were housed in groups of five at 22 to 24°C on a 12-h:12-h light-dark cycle; food and water were provided ad libitum. Animal protocols used in these studies were reviewed and approved by the Institutional Animal Care and Use Committee of the University of Illinois at Chicago. All animal procedures were conducted in accordance with the *Guide for the Care and Use of Laboratory Animals* (National Institutes of Health).

Total RNA Extraction and Real-Time PCR

Wound samples stored in RNAlater solution (Sigma) were homogenized in TRIzol reagent (Invitrogen, Carlsbad, CA). Total RNA was isolated and treated with DNase I according to the Invitrogen protocol and checked for purity, and its concentration was quantified spectrophotometrically. Total RNA (1 μg) was reverse transcribed to cDNA using the RETROscript RT kit (Invitrogen). GAPDH primers were published previously (20). Spry2 primers were designed using SciTools PrimerQuest software (Integrated DNA Technologies, Coralville, IA); Spry2 primer sequences were as follows: forward, 5′-ACTGCTCCAATGACGATGAGGACA-3′; and reverse, 5′-CCTGGCACAATTTAAGGCAACCCT-3′. cDNA samples, upstream and downstream primers for both the endogenous control gene (GAPDH) and the target gene (Spry2), and SYBR Green PCR Master Mix (Applied Biosystems, Foster City, CA) were loaded onto MicroAmp 96-well PCR reaction plates (Applied Biosystems), and the amplification protocol was run using the ABI Prism 7000 and StepOnePlus Real-Time PCR systems (Applied Biosystems). Raw threshold cycle (C_t) data were analyzed using the $\Delta\Delta C_t$ method, as previously described (18). Values generated for each sample are normalized to GAPDH at each time point, and the data are expressed as fold increases in gene expression relative to normal, unwounded skin. Relative RNA expression was subjected to statistical analysis by one-way ANOVA and Bonferroni's posttests using GraphPad Prism 4.0 software (GraphPad Software, San Diego, CA).

Protein Extraction and Western Blot Analysis

Wound samples (3 mm) that had been kept frozen at −80°C were homogenized in 500 μl of radioimmunoprecipitation assay buffer with a protease inhibitor cocktail (1/100 dilution; Sigma). Samples were centrifuged at 13,000 rpm at 4°C for 15 min. The resulting supernatants were collected, and the protein concentrations were quantified using a BCA protein assay kit (Pierce, Rockford, IL). Protein extracts were mixed with SDS-PAGE buffer and 2-mercaptoethanol (5% of total) and boiled for 3 min. Protein samples (30–55 μg per lane) were loaded into corresponding wells in a 10% Tris-glycine acrylamide gel (Bio-Rad, Hercules, CA). Separated proteins were transferred to a nitrocellulose membrane and blocked with 5% skim milk in Tris-buffered saline. Antibodies were applied to the membrane for 1 h and washed with Tris-buffered saline-Tween 20. For the study for Spry2 presence, rabbit anti-human Spry2 (1/500; Sigma) was used. For the study for MAPK signaling proteins, rabbit anti-rat p44/42 MAPK [total (t)-Erk1/2; Cell Signaling Technology, Danvers, MA] or rabbit anti-rat phospho-p44/42 MAPK [phospho (p)-Erk1/2; Cell Signaling Technology] was used. Rabbit anti-human α-tubulin (1/3,000; Abcam, Cambridge, MA) was used as a loading control for both studies. Finally, the membrane was incubated with goat anti-rabbit horseradish peroxidase (1/2,000; Bio-Rad), followed by enhanced chemiluminescence for the detection of positive bands. Imaging and relative protein quantification of the resulting membranes were obtained using ChemiDoc (Bio-Rad).

Endothelial Cell Culture: Migration and MAPK Activation

Recombinant, cell permeable, TAT-tagged green fluorescent protein (GFP), human (h)Spry2, and dominant-negative mutant of Spry2 (Y55F) used in the described experiments were expressed and purified as described previously (45, 46).

Cell migration. Mouse embryonic ECs (MEECs) (gift from Dr. Cuevas, Loyola University, Chicago, IL) were maintained in Dulbecco's modified Eagle's medium containing 3% fetal bovine serum (FBS) and incubated at 37°C in a humidified atmosphere of 5% CO_2-95% room air. Cells were grown to confluency in a 96-well cell culture plate (25,000 cells/well) and serum starved for 5 h. Cells were pretreated for 5 h with 20 μg/ml each of TAT-GFP (control), TAT-Spry2, or TAT-Spry2^{Y55F} before introducing a wound into the monolayer with a 10-μl pipette tip. Cells were washed once with serum-free media, and the TAT protein-containing media was returned to the respective wells. FBS (10%) was added to induce the migration of cells in one group; another group of cells was not treated with FBS. The same fields were photographed 15 h after FBS treatment, and scratch widths were measured using Photoshop software (Adobe Systems, San Jose, CA). Scratches were photographed with a Nikon

(Tokyo, Japan) digital camera mounted on an Olympus CKX41 culture microscope (Olympus, Center Valley, PA). Percent closure measurements were subjected to statistical analysis by one-way ANOVA and Bonferroni's posttests using GraphPad Prism 4.0 software (GraphPad Software).

MAPK activation. Human umbilical vein ECs (HUVECs) (gift from Dr. Greisler, Loyola University) were seeded onto 1 μg/cm^2 fibronectin-coated flasks and maintained in basal endothelial growth medium-2 (EGM-2) supplemented with 2% (vol/vol) FBS, 0.04% hydrocortisone, 0.4% hFGF-B, 0.1% VEGF, 0.1% R3-human insulin-like growth factor-1, 0.1% ascorbic acid, 0.1% human epidermal growth factor, 0.05% gentamicin, 0.05% amphotericin-B, and 0.1% heparin (EGM-2 BulletKit CC-3162; Lonza, Basel, Switzerland) at 37°C and 5% CO_2-95% room air. HUVECs (10^5 cells/35 mm dish) were serum starved in EGM-2 medium containing 0.1% FBS overnight and exposed to 10 μg/ml each of TAT-GFP (control), TAT-Spry2, or TAT-Spry2^{Y55F} for 1 h at 37°C. The cells were then stimulated with VEGF (50 ng/ml; Millipore, Billerica, MA) for 10 or 30 min and lysed in SDS sample buffer. Protein concentrations were determined, and equal amounts of protein were analyzed by Western blot analysis. Nitrocellulose membranes were immunoblotted with mouse monoclonal phospho-p44/42 MAPK antibody (p-ERK1/2; Cell Signaling Technology), and after being stripped, the blots were reprobed with rabbit polyclonal Erk1/2 antibody (Millipore). TAT-tagged proteins were detected by anti-hemagglutinin peroxidase (Roche, Indianapolis, IN) antibodies, as previously described (45).

Treatment of Wounds with Recombinant Proteins

FVB mice were wounded, as described. At *day 5* postinjury, 20 μl of controlled-release gel containing 2 μg of recombinant, cell permeable, TAT-tagged GFP (control), hSpry2, or dominant-negative Spry2^{Y55F} mutant was applied onto each 3-mm wound and covered with Tegaderm dressing (3M, St. Paul, MN). Pluronic gel (25%) was prepared by mixing Pluronic F-127 powder (Sigma) with a 20 mM HEPES, 150 mM NaCl, and 10% glycerol buffer at pH 8.0; the mixture is liquid below 15°C and gelatinous above 20°C (17, 28). Wound samples were harvested 10 days postinjury; three were placed in OCT compound (Sakura Finetechnical) for immunofluorescent histochemistry, and three were snap frozen for Western blot analysis.

Immunofluorescent Histochemistry

Frozen samples in OCT compound were sectioned at 8-μm thickness, with five sections per slide. Wound sections were air dried for 10 min, rehydrated in PBS for 10 min, and fixed in precooled acetone for 10 min. After being washed with 1× PBS two times for 3 min, the sections were first blocked using normal goat serum (1/10 dilution; Sigma) to prevent nonspecific binding of secondary antibody, followed by a 3 min of 1× PBS wash. For Spry2 localization studies, the slides were stained using polyclonal rabbit anti-human Spry2 primary antibody (1/200; Rockland Immunochemicals, Gilbertsville, PA) or rabbit IgG negative control (1/1,200; Vector, Burlingame, CA), followed by Alexa Fluor 488 goat anti-rabbit IgG fluorescent secondary antibody (1/500; Invitrogen). The specificity of the anti-Spry2 antibody in wounded and unwounded murine skin tissue was assessed by the preabsorption of anti-Spry2 with a recombinant peptide specific to the antibody, as previously described (46). Serial cryosections of normal, unwounded skin and skin 14 days postinjury were incubated with neutralized or nonneutralized anti-Spry2, or with an IgG isotype control, followed by Alexa Fluor 488 fluorescent secondary antibody. For wound vascularity studies, the slides were stained using purified rat anti-mouse CD31 (platelet endothelial cell adhesion molecule-1) primary antibody (1/100; BD Pharmingen, San Diego, CA) or rat IgG negative control (1/20; BD Pharmingen), followed by Alexa Fluor 594 goat anti-rat IgG fluorescent secondary antibody (1/1,000; Invitrogen). After each 45-min incubation with primary and secondary antibodies, the slides were washed for 3 min, three times, in 1× PBS (pH 7.4) and mounted in 50% glycerol in PBS. All incubations and washes were performed at room temperature. Slides were visualized and the staining quantified using Scion Image (Scion, Frederick, MD). For Spry2 localization studies, images of sections taken at 20× magnification were sorted into "wound bed" and "margin" categories based on anatomical features. Spry2-positive cells were counted by two investigators, and the results were normalized to wound area and averaged. For wound vascularity studies, a quantification of CD31 (platelet endothelial cell adhesion molecule-1) staining was performed as previously described (41). Relative Spry2 and CD31 expressions were subjected to statistical analysis by one-way ANOVA and Bonferroni's posttests using GraphPad Prism 4.0 software (GraphPad Software).

RESULTS

Spry2 mRNA Expression and Protein Production in Murine Skin Wounds During Healing

To determine whether Spry2 may play a significant role in the process of murine excisional skin wound healing, a time course study of Spry2 levels in the wound was performed. We followed the experimental design of previous studies that investigated healing in a well-established murine 3-mm excisional dermal wound model (40) and examined Spry2 mRNA and protein levels at eight time points postwounding: 1, 3, 5, 7, 10, 14, 21, and 28 days. These time points have been found to correlate with defined stages of the healing process in this wound model: epithelial closure is complete by *day 5* postwounding, whereas collagen content and vascularity peak at *day 10* (40). Whole wound samples were harvested at these time points and analyzed for the presence and relative expression of Spry2.

Spry2 mRNA expression was analyzed using real-time RT-PCR. The amount of Spry2 mRNA relative to normal, unwounded skin was normalized to the GAPDH endogenous control at each time point. Relative levels of Spry2 mRNA were stable until *day 5*, after which they began to increase: at *day 10* a 1.7-fold increase was observed, and at *day 14* Spry2 mRNA levels increased 3.1-fold relative to unwounded skin (Fig. 1*A*, $P < 0.05$). Spry2 mRNA expression peaked at *day 14* postinjury and then gradually decreased to the approximate level observed at *day 10* during the last two time points that were investigated (*days 21* and *28*, Fig. 1*A*).

To determine whether time course levels of Spry2 protein are similar to the mRNA expression that was observed, the protein content of Spry2 in whole wound samples was examined using Western blot analysis. Little to no Spry2 was detected in normal, unwounded skin and during the earliest time points until *day 5* postwounding. Spry2 protein levels then increased until *day 14*, after which they were observed to decrease (Fig. 1*B*). This temporal pattern of Spry2 content is similar to that observed in our mRNA expression study (Fig. 1*A*), indicating that Spry2 production increases dramatically during the post-proliferative stage of wound healing.

Spry2-Positive Cell Numbers Increase in the Wound Bed During Healing

Having elucidated the general pattern of Spry2 production in whole wound samples over the time course of murine excisional skin wound healing, we sought to localize the protein in the wound. Assessment of Spry2 antibody specificity by peptide preabsorption showed that, both in wounded as well as in

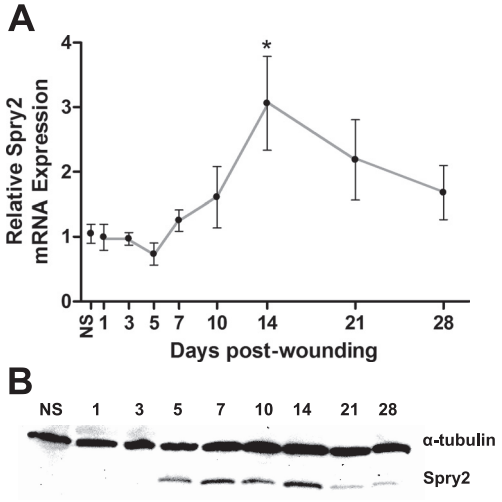

Fig. 1. Sprouty 2 (Spry2) mRNA expression and protein levels in mouse skin wounds during healing. Wound samples were harvested at 8 time points following 3-mm dermal excisional punch biopsy and subjected to biochemical analysis. *A:* Spry2 mRNA transcript abundance was measured using real-time RT-PCR, normalized to GAPDH endogenous control at each time point, and compared with normal, unwounded skin (NS). Data are expressed as means ± SE; $n = 5$ for all time points except *day 10* ($n = 4$). *$P < 0.05$ at *day 14* vs. NS, when a peak in Spry2 mRNA is observed, by one-way ANOVA and Bonferroni's posttest. *B:* Western blot analysis shows that Spry2 protein levels follow the general pattern of Spry2 mRNA expression during wound healing. Separated bands were visualized using anti-human Spry2 and anti-α-tubulin antibodies. α-Tubulin was used as a loading control. Representative blot is from four independent experiments with similar results.

unwounded skin, Spry2 was positively expressed only in the dermis of murine skin; autofluorescence of the epidermis was observed in the neutralized antibody and isotype controls (supplemental figure). Immunofluorescent histochemical analysis for Spry2-positive cells was performed on 20× magnification fields from the wound bed and wound margin. Whereas Spry2-positive cell numbers in the wound margin did not change over the course of healing (Fig. 2*A*, *bottom*), Spry2-positive cell numbers increased dramatically after *day 7* in the wound bed (Fig. 2*B*). In the wound bed, a 17.1-fold increase in Spry2-expressing cells was observed on *day 28* compared with *day 7* postinjury (Fig. 2*A*, *top*, $P < 0.05$). These results suggest that the number of cells in the dermis of the wound bed that produce Spry2 increases during the later stages of healing up to levels observed in normal, unwounded skin (Fig. 2*A*, *top*, NS vs. *day 28*), whereas the number of Spry2-producing cells in the dermis of the wound margin remains unchanged during healing from the levels observed in unwounded skin (Fig. 2*A*, *bottom*, NS vs. all time points).

All results up to this point show a specific profile of Spry2 production during the time course of murine excisional dermal wound repair. During the inflammatory and early proliferative phases of wound healing when VEGF levels are at their highest and when angiogenesis is occurring at a rapid rate (40), Spry2 production and Spry2-producing cells are at very low levels. During the post-proliferative phase when vascularity is known to peak and subsequently subside (40), Spry2 production peaks, whereas Spry2-producing cells increase in the dermis of the wound bed.

Endothelial Cell Migration and MAPK Signaling Are Inhibited Following Incubation with Recombinant TAT-Tagged Spry2

Having found that Spry2 production changes considerably in the wound bed during the time course of dermal healing and that its expression correlates with the known angiogenic profile in this wound model (40), we sought a method of modulating Spry2 levels in the wound so as to determine whether Spry2 has a function in regulating angiogenesis. A simple exogenous application of recombinant Spry2 is unlikely to elicit a biological response because Spry proteins are intracellular and known to function by binding to intracellular MAPK-associated signaling proteins. We have previously developed an experimental method of modifying

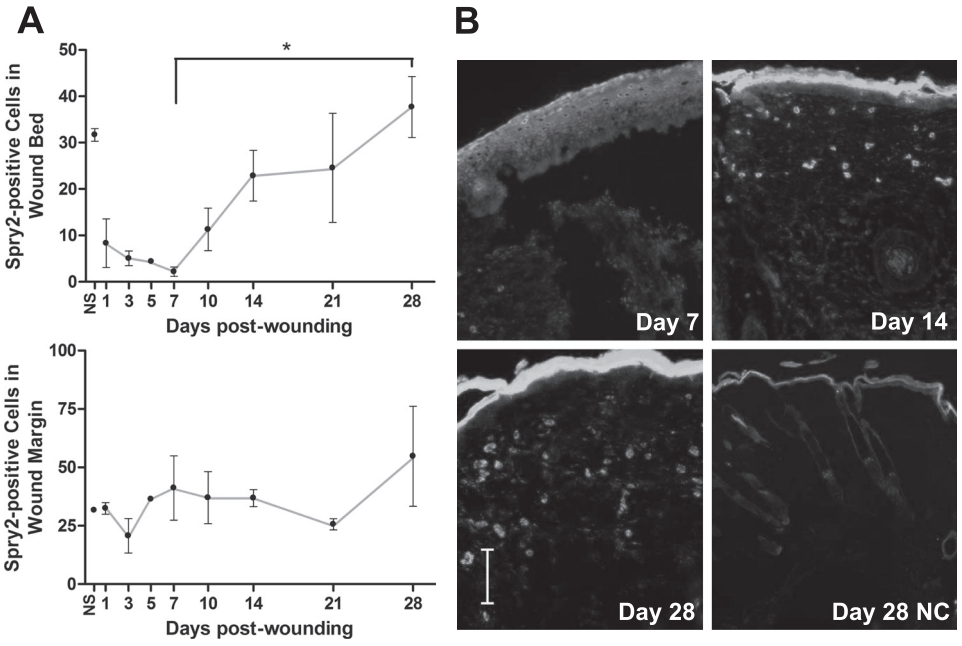

Fig. 2. Spry2-positive cell numbers increase in the dermis of the wound bed during healing. Immunofluorescent histochemical analysis for Spry2 was performed on cryosections from whole wound samples following harvest at 8 time points after 3-mm dermal excisional punch biopsy. *A:* quantification of Spry2-positive cells in the wound bed *(top)* and wound margin *(bottom)*. Data are expressed as means ± SE; $n = 3$ for all time points except *days 1* and *5* ($n = 2$) and *day 10* ($n = 4$). *$P < 0.05$ at *day 28* vs. *day 7* in the wound bed by one-way ANOVA and Bonferroni's posttest. *B:* representative photomicrographs of Spry2-positive immunofluorescence in the dermis of the wound bed from *days 7*, *14*, and *28* postwounding; a negative control (NC) using a rabbit IgG primary antibody from a *day 28* wound is shown. Scale bar = 50 μm.

recombinant Spry2 with a transduction domain derived from the human immunodeficiency virus TAT protein so as to make Spry2 cell permeable, but this work was done using HeLa cancer cells (45) and VSMCs (46), not ECs. Therefore, it was important to establish the efficacy of TAT-tagged Spry2 on EC migration and Raf/Mek/Erk signaling pathway activation in vitro before making conclusions about the effect of TAT-tagged Spry2 on angiogenesis in vivo.

To assess EC migration, MEECs were pretreated with TAT-GFP, TAT-Spry2, or TAT-tagged dominant-negative mutant of Spry2 (TAT-Spry2^{Y55F}) before introducing a wound into the monolayer. Scratch wounds made on MEECs not exposed to FBS exhibited very low closure rates and no significant differences were seen between TAT protein-treated groups 15 h after injury (Fig. 3*A*, *left*). Cell migration was dramatically induced by FBS in MEECs pretreated with TAT-GFP and TAT-Spry2^{Y55F}; cells treated with the dominant-negative Y55F mutant of Spry2 showed a slight but not significant increase in closure relative to the GFP-treated control group (Fig. 3*A*, *right*). In contrast, MEECs pretreated with TAT-Spry2 exhibited significantly reduced scratch wound closures compared with the TAT-GFP-treated controls (Fig. 3*A*, *right*, $P < 0.01$), suggesting that TAT-tagged Spry2 successfully permeated the MEEC membranes to inhibit their migration ability in response to serum.

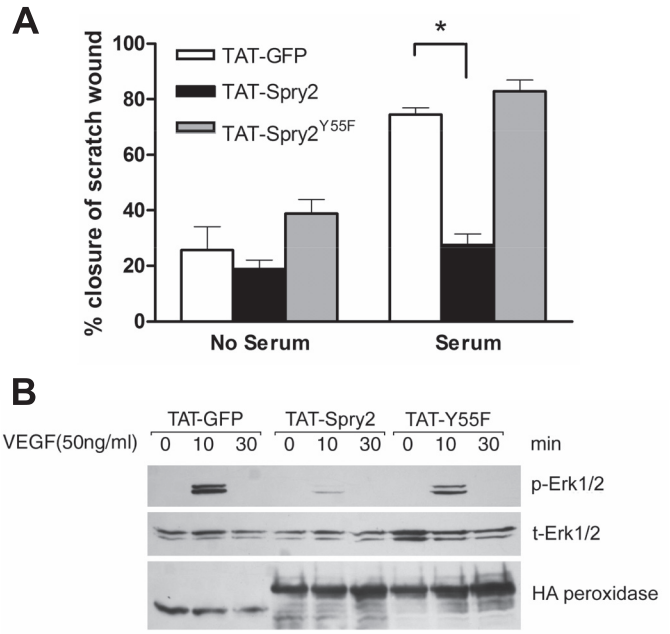

Fig. 3. Endothelial cell (EC) migration and mitogen-activated protein kinase (MAPK) signaling are inhibited following incubation with recombinant transactivator of transcription (TAT)-tagged Spry2. *A:* TAT-Spry2 inhibits the migration of mouse embryonic ECs in response to serum. Mouse embryonic ECs grown to confluency were pretreated with 20 μg/ml of TAT-proteins for 5 h before making scratch wounds and monitoring cell migration in response to serum (10%) while in the presence of TAT proteins, as described in MATERIALS AND METHODS. Marked fields were photographed at *time 0* and 15 h after making the scratches, and migration of cells was calculated as percent closure of scratch wound. The mean ± SE of 2 separate experiments is shown. *$P < 0.01$ for Spry2 vs. green fluorescent protein (GFP) in the serum group by one-way ANOVA and Bonferroni's posttest. *B:* TAT-Spry2 inhibits MAPK signaling of human umbilical vein ECs in response to vascular endothelial growth factor (VEGF). Human umbilical vein ECs were serum starved in endothelium growth medium-2 containing 0.1% FBS overnight and pretreated with 10 μg/ml each of TAT-GFP, TAT-Spry2, or TAT-Spry2^{Y55F} for 1 h at 37°C before incubating with VEGF (50 ng/ml) for 10 or 30 min. Total cell lysates were subjected to SDS-PAGE and immunoblotted with anti-phospho-Erk1/2 (p-Erk1/2), anti-total Erk1/2 (t-Erk1/2), and anti-hemagglutinin (HA)-peroxidase (to detect TAT-tagged proteins)-conjugated antibodies.

To assess EC MAPK activation, human umbilical vein ECs (HUVECs) were pretreated with TAT-GFP, TAT-Spry2, or TAT-Spry2^{Y55F}, incubated with VEGF for 10 or 30 min, and analyzed via Western blot analysis for the presence of t-Erk1/2 and p-Erk1/2 signaling proteins. As predicted, the level of t-Erk1/2 was relatively unchanged across all treatment groups (Fig. 3*B*, t-Erk1/2). A decrease in p-Erk1/2 was observed in TAT-Spry2-treated HUVECs relative to the TAT-GFP-treated cells after 10 min of VEGF incubation; no p-Erk1/2 was detected in HUVECs not incubated with VEGF nor in those incubated with VEGF for 30 min (Fig. 3*B*, p-Erk1/2). However, TAT-Spry2^{Y55F}-treated HUVECs did not exhibit an increase in p-Erk1/2 content relative to the TAT-GFP treated controls (Fig. 3*B*, p-Erk1/2). Positive hemagglutinin peroxidase staining confirmed the presence of TAT-tagged proteins in cell cultures after treatment. These results suggest that TAT-tagged Spry2 successfully permeated the HUVEC membranes to inhibit their Raf/Mek/Erk signaling pathway activation in response to VEGF stimulation. Thus cell permeable TAT-Spry2 is an effective treatment for the downregulation of important angiogenesis-related functions in ECs.

Wound Vascularity Is Decreased Following Exogenous Application of Recombinant TAT-Tagged Spry2

To test the hypothesis that Spry2 functions to downregulate angiogenesis during murine dermal wound repair, controlled-release gel containing recombinant, cell permeable, TAT-tagged GFP (control), Spry2, or dominant-negative mutant of Spry2 (Y55F) proteins was exogenously applied to wounds at *day 5* after injury. *Day 5* was chosen as the time point for treatment because it correlates with the peak production of VEGF as well as the onset of angiogenesis in this wound model (40). Whole wound samples were harvested at *day 10* postinjury [a time point that correlates with a peak in wound vascularity in this model (40)] and analyzed via immunofluorescent histochemistry for the EC marker CD31. An abundance of CD31 correlates with blood vessel density and is thus an experimental measure of angiogenesis (40). The CD31 area in the wound was significantly decreased by 30% in Spry2-treated wounds relative to the GFP-treated controls (Fig. 4*B*, $P = 0.05$). Wounds treated with the dominant-negative mutant of Spry2 (Y55F) exhibited a moderate (15%) increase in CD31 expression in the wound compared with the GFP-treated controls (Fig. 4). This result is consistent with previous data that showed that the Spry2^{Y55F} mutant acts as a dominant negative and reverses the inhibitory functions of endogenous Spry2 (23, 30, 38). Overall, these results indicate that Spry2 functions to downregulate vascularity in the healing murine wound and that adding more of the protein to the wound during the proliferative phase of wound repair significantly promotes this antiangiogenic phenotype.

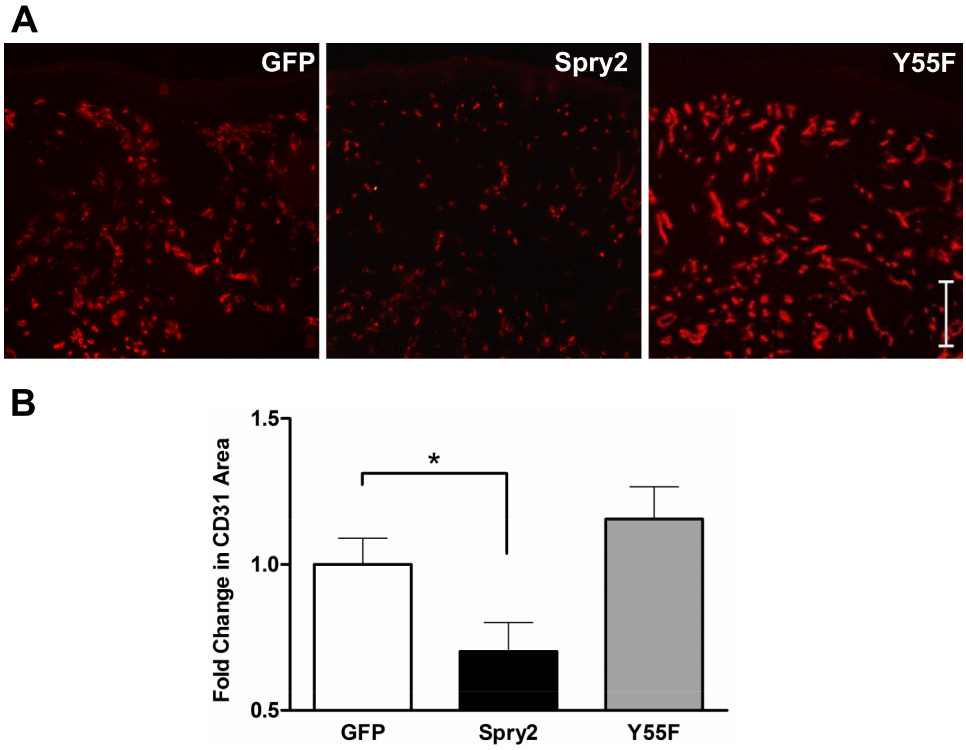

Fig. 4. Wound vascularity is decreased following exogenous application of recombinant TAT-tagged Spry2. Immunofluorescent histochemical analysis for EC marker CD31 (platelet EC adhesion molecule-1) was performed on cryosections from whole wound samples harvested at *day 10* postinjury from 3-mm dermal excisional punch biopsy and after exogenous application at *day 5* postwounding of controlled-release gel containing 2 μg of recombinant cell-permeable, TAT-tagged GFP (control), Spry2, or dominant-negative mutant of Spry2 (Y55F) (n = 6 for GFP, n = 5 for Spry2, and n = 6 for Spry2^{Y55F}). *A:* representative photomicrographs of CD31-positive immunofluorescence in GFP-, Spry2-, and Spry2^{Y55F}-treated wounds. Scale bar = 50 μm. *B:* quantification of CD31 immunofluorescence shows a moderate increase in vascularity in Spry2^{Y55F}-treated wounds and a significant decrease in vascularity in Spry2-treated wounds relative to the GFP-treated control group. Percent CD31 area per field was normalized and compared with the GFP control group to yield fold change in CD31 area; data are expressed as means ± SE. *P = 0.05 for Spry2 vs. GFP by one-way ANOVA and Bonferroni's posttest.

MAPK Signaling Is Decreased in TAT-Spry2-Treated Wounds, Whereas TAT-Spry2^{Y55F}-Treated Wounds Exhibit Increased MAPK Signaling

We next assessed whether the observed decrease in wound vascularity after Spry2 treatment is concurrent with an inhibition of the Raf/Mek/Erk signaling pathway in vivo. The levels of total Erk1/2 and p-Erk1/2 signaling proteins were determined by Western blot analyses of whole wound tissue samples harvested at *day 10* postinjury, following an exogenous application at *day 5* postinjury of recombinant, TAT-tagged GFP control, TAT-Spry2, or TAT- Spry2^{Y55F}. As predicted, the level of total Erk1/2 was relatively unchanged across all treatment groups (Fig. 5*B*, t-Erk1/2). A decrease in p-Erk1/2 was observed in Spry2-treated wounds relative to the GFP-treated control group; in contrast, Spry2^{Y55F}-treated wounds exhibited an increase in p-Erk1/2 content (Fig. 5*A*, p-Erk1/2). These results suggest that Spry2 may inhibit the MAPK signaling pathway during murine excisional skin wound healing simultaneously with a downregulation in angiogenesis.

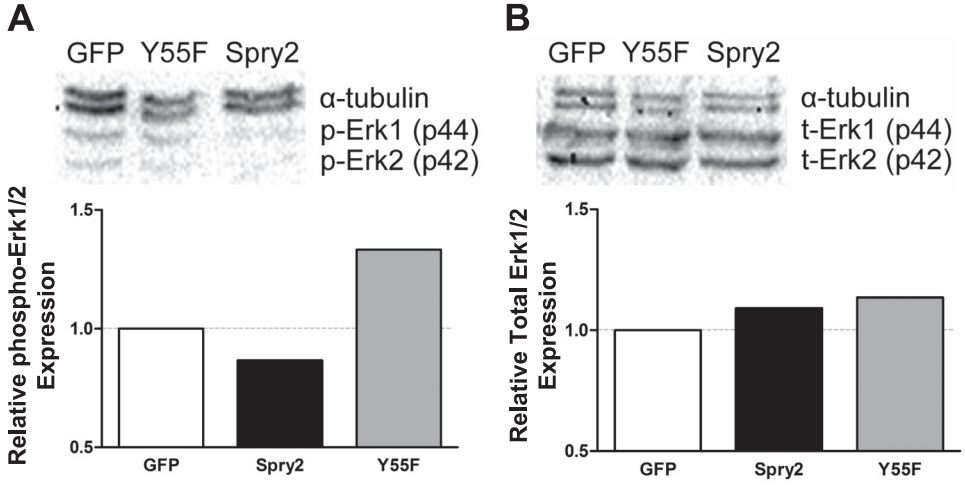

Fig. 5. MAPK signaling is decreased in TAT-Spry2-treated wounds, whereas TAT-Spry2^{Y55F}-treated wounds exhibit increased MAPK signaling. Levels of signaling proteins were analyzed by Western blot analysis performed on whole wound samples harvested at *day 10* postinjury from 3-mm dermal excisional punch biopsy and after exogenous treatment with TAT-tagged recombinant proteins at *day 5* postwounding. Data represent results from 1 of 4 independent experiments with similar results. *A* and *B*, *top*: representative Western blots showing expression of p-Erk1/2 (*A*) and t-Erk1/2 (*B*) signaling proteins in GFP-, Spry2^{Y55F}-, Spry2-treated wounds. α-Tubulin was used as a loading control. *A* and *B*, *bottom*: quantification of respective Western blots showing p-Erk1/2 (*A*) and t-Erk1/2 (*B*) protein expression normalized to α-tubulin and compared with the GFP control group.

DISCUSSION

This is the first study to characterize Spry protein production and function in the context of in vivo wound repair and wound angiogenesis. We show that Spry2 mRNA and protein levels increased significantly during the post-proliferative phase of healing, coincident with the onset of vascular regression in this model. Spry2 production was localized to cells in the dermis of the wound bed where angiogenesis is known to occur during wound healing. The application of exogenous, cell-permeable Spry2 to the wound during the angiogenic phase of healing

significantly reduced vessel density and simultaneously reduced MAPK signaling. These results indicate that endogenous Spry2 may function to downregulate angiogenesis in the healing murine skin wound, potentially by inhibiting the MAPK signaling pathway.

Spry is a negative feedback loop inhibitor of RTK-associated signaling pathways that converge in the Raf/Mek/Erk pathway and are known to promote cellular changes associated with angiogenesis in ECs (Fig. 6). Three RTK ligands known to be proangiogenic in the context of wound repair are FGF-2, PDGF, and VEGF.

Upon injury, sequestered FGF-2 is released into the wound environment and soluble FGF-2 is capable of stimulating early angiogenic events, including the proliferation and migration of ECs for blood vessel sprouting, as well as inducing the production of VEGF (32, 33). Previous studies in our laboratory show that FGF-2 production is increased progressively following 3-mm excisional skin injury in the murine model (40). PDGF is released by the degranulation of platelets and has been shown to be proangiogenic during wound healing by inducing the production of VEGF and particularly by promoting the maturation of blood vessels via the recruitment of pericytes and VSMCs (5). While keratinocytes are known to produce basal levels of VEGF in uninjured skin (4, 13), there is no VEGF present in the wound site immediately after injury (33, 40). The production of VEGF is induced by hypoxia (12) in the early phases of wound repair, and previous studies in our laboratory show that VEGF production peaks 5 days postinjury in the 3-mm excisional skin wound model (40).

Thus soluble FGF-2, PDGF, and VEGF are all present and active in the wound during the proliferative phase of healing. Their binding to respective RTKs may trigger not only the propagation of the proangiogenic Raf/Mek/Erk pathway initially but also the production and activation of Spry2 intracellularly in ECs and VSMCs. Indeed, growth factors have been shown to increase Spry2 expression (10, 22, 34), and the elevation in Spry2 content may inhibit the ability of RTKs to further activate the Raf/Mek/Erk signaling pathway, resulting in the eventual downregulation of proangiogenic cellular behavior (Fig. 6).

Previous work in our laboratory (40) has shown that blood vessel density peaks at *day 10* postinjury in murine 3-mm excisional skin wounds. Starting at *day 14*, relative vessel density begins to decrease and regression occurs (40). The temporal pattern of Spry2 production that we observed in this wound model correlates with this pattern of angiogenesis, in that Spry2 mRNA and protein levels were seen to peak at *day 14* postwounding. Furthermore, the numbers of Spry2-producing cells in the dermis of the wound bed increased after *day 7* postinjury. Importantly, the current studies showed that Spry2 functions to inhibit in vivo angiogenesis as well as MAPK signaling in the murine dermal wound. These findings are strongly supported by the observation that both angiogenesis and MAPK signaling were moderately upregulated following the addition of the dominant-negative mutant of Spry2 to the wounds. The Spry2^{Y55F} mutant is thought to function by forming heterodimers with endogenous Spry2 and interfering with the binding of endogenous Spry2 to its targets in the MAPK pathways, thereby promoting the opposite phenotype of the wild-type protein (Fig. 6) (23, 30, 38). Interestingly, we observed marginal stimulatory effects of Spry2^{Y55F} on in vitro EC migration and MAPK activation; one potential reason for this result is the relatively low endogenous production of wild-type Spry2 (to which the Spry2 mutant can bind and

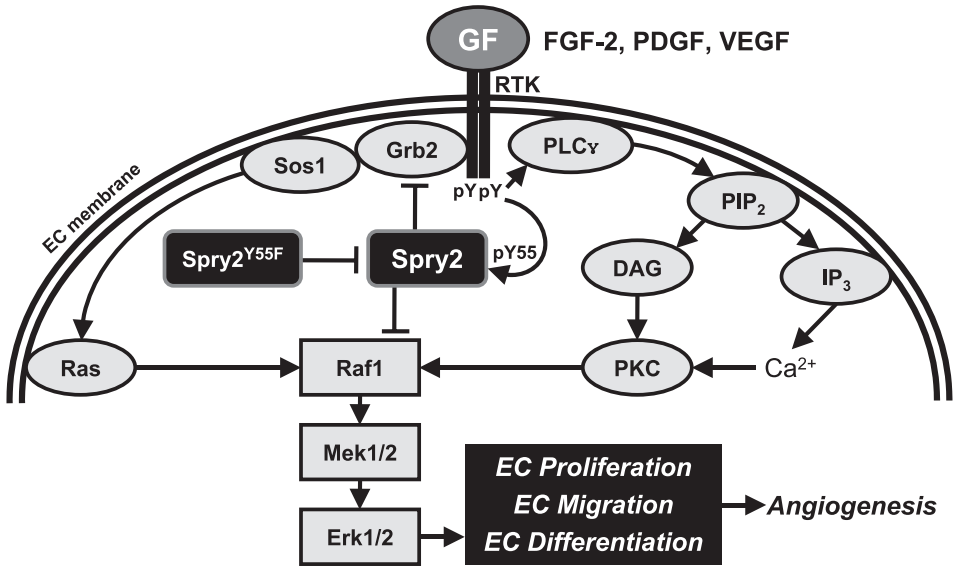

Fig. 6. Spry2 and Spry2^{Y55F} function in the context of EC MAPK signaling. Upon growth factor (GF) binding to its respective receptor tyrosine kinase (RTK) and activation of the respective signaling pathway, Spry2 is induced to translocate to the inner plasma membrane where it gets activated (in many cases via phosphorylation on the Y55 by a Src-like kinase) and functions by interacting with various MAPK signaling pathway-associated proteins in a GF-specific manner. When RTK signaling is Ras dependent (*left*), Spry2 inhibition of this pathway is thought to occur at the level of GF receptor-bound protein-2 (Grb2) or Raf1. When RTK signaling is Ras independent (*right*), Spry2 inhibition of this pathway is thought to occur at the level of Raf1. In many cases, pY55 is required for Spry2 inhibition of the Raf/Mek/Erk pathway. The dominant-negative Y55F mutant of Spry2 inhibits endogenous Spry2 action, thereby promoting the Raf/Mek/Erk pathway. FGF-2, fibroblast GF-2; PDGF, platelet-derived GF; pY, phosphorylated tyrosine; Sos1, son of sevenless-1; PLC-γ, phospholipase C-γ; PIP_2, phosphatidylinositol bisphosphate; DAG, diacylglycerol; IP_3, inositol trisphosphate; PKC, protein kinase C. Information in this figure was compiled from Refs. 10, 16, 22, 23, 24, 27, 30, 34, 38.

inhibit) by EC cultures in response to a single controlled stimulus compared with the in vivo wound environment where multiple stimuli are involved.

The function of Spry2 in wound healing that is described here is consistent with two other in vivo models of murine angiogenesis, namely, embryo and hindlimb ischemia (26, 43). Our in vitro data using TAT-tagged Spry2 are also consistent with other EC culture studies (24, 26). The previous and current data support the conclusion that Spry2 downregulates angiogenesis during wound repair via its inhibitory action on the FGF-2-, PDGF-, and VEGF-stimulated Raf/Mek/Erk signaling pathway in ECs and VSMCs.

The mechanisms that drive blood vessel formation in physiological and pathological wound models have been the topic of much investigation; however, the mechanisms of angiogenic downregulation and subsequent vessel regression in the context of wound healing are not well understood. VEGF levels decrease in the resolving wound (40), and this simple loss of proangiogenic and vessel survival signals has been suggested to be the major cause of vascular regression (1). Recent studies in our laboratory demonstrate that late-phase exogenous administration of supraphysiological levels of the proangiogenic factors, including VEGF, FGF-2, and PDGF, cannot prevent vessel regression in the wound (21). These data suggest that active antiangiogenic signals, which strongly counteract the proangiogenic stimuli, may be present in the resolving wound. Thus, at any particular time point in healing, the balance between pro- and antiangiogenic factors favors one phenotype over the other (15), with the local environment of the resolving wound critically favoring the mechanisms that lead to angiogenic downregulation and subsequent blood vessel regression.

Many antiangiogenic factors have been identified in studies that focus on controlling the pathological angiogenesis that occurs in tumors (11) and in ocular neovascularization (3), but no such extensive analysis is yet available for the healing wound. Only thrombospondins (TSP) (25) and most recently interferon-inducible protein 10 (IP-10), also known as CXCL10 (7), have been implicated as endogenous physiological inhibitors of angiogenesis in the context of wound repair. In this study we identify Spry2 as another endogenous antiangiogenic agent present and active in the resolving dermal wound.

TSP1/2 have both been implicated in downregulating wound angiogenesis (8, 25). IP-10, a CXCR3 ligand, has been shown to actively promote wound blood vessel regression even in the presence of proangiogenic factors (7). Given the documented roles for TSP and IP-10, it seems clear that Spry2 accounts for only a part of the late-phase regulatory mechanism of wound angiogenesis.

TSP and IP-10 molecules are extracellular mediators of angiogenesis. TSP2 and IP-10 are both expressed during the later stages of wound repair and function to inhibit angiogenesis and even promote vascular regression via extracellular binding to ECs. Although Spry2 is expressed during similar time points during wound healing, it functions to downregulate angiogenesis in an intracellular fashion (Fig. 6). By inhibiting the potentiation of RTK-stimulated proangiogenic MAPK signaling pathways, Spry2 may contribute to the shift in the balance between pro- and antiangiogenic stimuli in ECs and VSMCs. This shift may make these cells more sensitive to extracellular antiangiogenic factors like TSP and IP-10, resulting in the observed phenotypes of wound blood vessel involution and eventual vascular homeostasis.

It is important to note that the current study investigated the function of one of four mammalian homologs of the Spry family of proteins. Given what is currently known about them (10, 16, 22, 26, 43), it is likely that Spry1 and especially Spry4 have analogous physiological functions to those described here for Spry2. The contributions of these and other Spry-related proteins, i.e., the Spred family (9), to the regulation of wound angiogenesis remain to be elucidated.

Overall, there is evidence of complex regulatory and compensatory mechanisms driven by endogenous antiangiogenic factors, both intra- and extracellular, all functioning to ensure the proper control of wound angiogenesis and the promotion of physiological blood vessel regression during wound repair. Studies of vascular regression in wounds are very likely to have applicability to multiple disease states. The failure of appropriate vascular regression has been implicated in pathological conditions such as cancer, inflammatory diseases like arthritis, some types of chronic wounds, and scarring (19, 36, 44). In contrast, an overinhibition of angiogenesis is characteristic of many poorly healing wounds, particularly in patients with diabetes (29), and is highly implicated in various cardiovascular diseases (35). Additional studies of the regulatory mechanisms that govern angiogenesis at sites of injury may ultimately assist in the development of novel effective therapeutic regimes to treat patients with dysfunctional neovascularization or vascular regression.

ACKNOWLEDGMENTS

We thank Francis Edwin, Wendy Cerny, Shujuan Guo, Ariel Johnson, Julia Tulley, and Anna Turabelidze for advice and support.

GRANTS

This work was supported by National Institutes of Health Grants R01-GM-50875 and P20-GM-078426 (to L. A. DiPietro), T32-DE-018381 (to L. A. DiPietro and M. S. Wietecha), T32-AA-013527 (to M. J. Ranzer), and R01-GM-073181 (to T. B. Patel) and by the University of Illinois at Chicago College of Dentistry Schour Scholars Fund.

DISCLOSURES

No conflicts of interest, financial or otherwise, are declared by the author(s).

REFERENCES

1. **Alon T, Hemo I, Itin A, Pe'er J, Stone J, Keshet E.** Vascular endothelial growth factor acts as a survival factor for newly formed retinal vessels and has implications for retinopathy of prematurity. *Nat Med* 1: 1024–1028, 1995.
2. **Antoine M, Wirz W, Tag CG, Mavituna M, Emans N, Korff T, Stoldt V, Gressner AM, Kiefer P.** Expression pattern of fibroblast growth factors (FGFs), their receptors and antagonists in primary endothelial cells and vascular smooth muscle cells. *Growth Factors* 23: 87–95, 2005.
3. **Azar DT.** Corneal angiogenic privilege: angiogenic and antiangiogenic factors in corneal avascularity, vasculogenesis, and wound healing (an American Ophthalmological Society thesis). *Trans Am Ophthalmol Soc* 104: 264–302, 2006.
4. **Ballaun C, Weninger W, Uthman A, Weich H, Tschachler E.** Human keratinocytes express the three major splice forms of vascular endothelial growth factor. *J Invest Dermatol* 104: 7–10, 1995.
5. **Barrientos S, Stojadinovic O, Golinko MS, Brem H, Tomic-Canic M.** Growth factors and cytokines in wound healing. *Wound Repair Regen* 16: 585–601, 2008.
6. **Bell SE, Mavila A, Salazar R, Bayless KJ, Kanagala S, Maxwell SA, Davis GE.** Differential gene expression during capillary morphogenesis in 3D collagen matrices: regulated expression of genes involved in basement

membrane matrix assembly, cell cycle progression, cellular differentiation and G-protein signaling. *J Cell Sci* 114: 2755–2773, 2001.
7. **Bodnar RJ, Yates CC, Rodgers ME, Du X, Wells A.** IP-10 induces dissociation of newly formed blood vessels. *J Cell Sci* 122: 2064–2077, 2009.
8. **Bornstein P.** Thrombospondins function as regulators of angiogenesis. *J Cell Commun Signal* 3: 189–200, 2009.
9. **Bundschu K, Walter U, Schuh K.** Getting a first clue about SPRED functions. *Bioessays* 29: 897–907, 2007.
10. **Cabrita MA, Christofori G.** Sprouty proteins, masterminds of receptor tyrosine kinase signaling. *Angiogenesis* 11: 53–62, 2008.
11. **Dass CR, Tran TM, Choong PF.** Angiogenesis inhibitors and the need for anti-angiogenic therapeutics. *J Dent Res* 86: 927–936, 2007.
12. **Detmar M, Brown LF, Berse B, Jackman RW, Elicker BM, Dvorak HF, Claffey KP.** Hypoxia regulates the expression of vascular permeability factor/vascular endothelial growth factor (VPF/VEGF) and its receptors in human skin. *J Invest Dermatol* 108: 263–268, 1997.
13. **Detmar M, Yeo KT, Nagy JA, Van de Water L, Brown LF, Berse B, Elicker BM, Ledbetter S, Dvorak HF.** Keratinocyte-derived vascular permeability factor (vascular endothelial growth factor) is a potent mitogen for dermal microvascular endothelial cells. *J Invest Dermatol* 105: 44–50, 1995.
14. **DiPietro LA, Nissen NN.** Angiogenic mediators in wound healing. In: *Angiogenesis: Models, Modulators, and Clinical Applications*, edited by Maragoudakis ME. New York: Plenum, 1998, p. 121–129.
15. **Distler JH, Hirth A, Kurowska-Stolarska M, Gay RE, Gay S, Distler O.** Angiogenic and angiostatic factors in the molecular control of angiogenesis. *Q J Nucl Med* 47: 149–161, 2003.
16. **Edwin F, Anderson K, Ying C, Patel TB.** Intermolecular interactions of Sprouty proteins and their implications in development and disease. *Mol Pharmacol* 76: 679–691, 2009.
17. **Escobar-Chavez JJ, Lopez-Cervantes M, Naik A, Kalia YN, Quintanar-Guerrero D, Ganem-Quintanar A.** Applications of thermo-reversible pluronic F-127 gels in pharmaceutical formulations. *J Pharm Pharm Sci* 9: 339–358, 2006.
18. **Fleige S, Walf V, Huch S, Prgomet C, Sehm J, Pfaffl MW.** Comparison of relative mRNA quantification models and the impact of RNA integrity in quantitative real-time RT-PCR. *Biotechnol Lett* 28: 1601–1613, 2006.
19. **Folkman J.** Angiogenesis in cancer, vascular, rheumatoid and other disease. *Nat Med* 1: 27–31, 1995.
20. **Giulietti A, Overbergh L, Valckx D, Decallonne B, Bouillon R, Mathieu C.** An overview of real-time quantitative PCR: applications to quantify cytokine gene expression. *Methods* 25: 386–401, 2001.
21. **Gosain A, Matthies AM, Dovi JV, Barbul A, Gamelli RL, DiPietro LA.** Exogenous pro-angiogenic stimuli cannot prevent physiologic vessel regression. *J Surg Res* 135: 218–225, 2006.
22. **Guy GR, Jackson RA, Yusoff P, Chow SY.** Sprouty proteins: modified modulators, matchmakers or missing links? *J Endocrinol* 203: 191–202, 2009.
23. **Hanafusa H, Torii S, Yasunaga T, Nishida E.** Sprouty1 and Sprouty2 provide a control mechanism for the Ras/MAPK signalling pathway. *Nat Cell Biol* 4: 850–858, 2002.
24. **Impagnatiello MA, Weitzer S, Gannon G, Compagni A, Cotten M, Christofori G.** Mammalian sprouty-1 and -2 are membrane-anchored phosphoprotein inhibitors of growth factor signaling in endothelial cells. *J Cell Biol* 152: 1087–1098, 2001.
25. **Kyriakides TR, Maclauchlan S.** The role of thrombospondins in wound healing, ischemia, and the foreign body reaction. *J Cell Commun Signal* 3: 215–225 2009.
26. **Lee SH, Schloss DJ, Jarvis L, Krasnow MA, Swain JL.** Inhibition of angiogenesis by a mouse sprouty protein. *J Biol Chem* 276: 4128–4133, 2001.
27. **Lim J, Wong ES, Ong SH, Yusoff P, Low BC, Guy GR.** Sprouty proteins are targeted to membrane ruffles upon growth factor receptor tyrosine kinase activation. Identification of a novel translocation domain. *J Biol Chem* 275: 32837–32845, 2000.
28. **Liu Y, Lu WL, Wang JC, Zhang X, Zhang H, Wang XQ, Zhou TY, Zhang Q.** Controlled delivery of recombinant hirudin based on thermosensitive Pluronic F127 hydrogel for subcutaneous administration: in vitro and in vivo characterization. *J Control Release* 117: 387–395, 2007.
29. **Martin A, Komada MR, Sane DC.** Abnormal angiogenesis in diabetes mellitus. *Med Res Rev* 23: 117–145, 2003.
30. **Mason JM, Morrison DJ, Bassit B, Dimri M, Band H, Licht JD, Gross I.** Tyrosine phosphorylation of Sprouty proteins regulates their ability to inhibit growth factor signaling: a dual feedback loop. *Mol Biol Cell* 15: 2176–2188, 2004.
31. **Minowada G, Jarvis LA, Chi CL, Neubuser A, Sun X, Hacohen N, Krasnow MA, Martin GR.** Vertebrate Sprouty genes are induced by FGF signaling and can cause chondrodysplasia when overexpressed. *Development* 126: 4465–4475, 1999.
32. **Nissen NN, Polverini PJ, Gamelli RL, DiPietro LA.** Basic fibroblast growth factor mediates angiogenic activity in early surgical wounds. *Surgery* 119: 457–465, 1996.
33. **Nissen NN, Polverini PJ, Koch AE, Volin MV, Gamelli RL, DiPietro LA.** Vascular endothelial growth factor mediates angiogenic activity during the proliferative phase of wound healing. *Am J Pathol* 152: 1445–1452, 1998.
34. **Ozaki K, Kadomoto R, Asato K, Tanimura S, Itoh N, Kohno M.** ERK pathway positively regulates the expression of Sprouty genes. *Biochem Biophys Res Commun* 285: 1084–1088, 2001.
35. **Pandya NM, Dhalla NS, Santani DD.** Angiogenesis—a new target for future therapy. *Vascul Pharmacol* 44: 265–274, 2006.
36. **Polverini PJ.** Angiogenesis in health and disease: insights into basic mechanisms and therapeutic opportunities. *J Dent Educ* 66: 962–975, 2002.
37. **Ribatti D, Nico B, Crivellato E.** Morphological and molecular aspects of physiological vascular morphogenesis. *Angiogenesis* 12: 101–111, 2009.
38. **Sasaki A, Taketomi T, Wakioka T, Kato R, Yoshimura A.** Identification of a dominant negative mutant of Sprouty that potentiates fibroblast growth factor- but not epidermal growth factor-induced ERK activation. *J Biol Chem* 276: 36804–36808, 2001.
39. **Shim K, Minowada G, Coling DE, Martin GR.** Sprouty2, a mouse deafness gene, regulates cell fate decisions in the auditory sensory epithelium by antagonizing FGF signaling. *Dev Cell* 8: 553–564, 2005.
40. **Swift ME, Kleinman HK, DiPietro LA.** Impaired wound repair and delayed angiogenesis in aged mice. *Lab Invest* 79: 1479–1487, 1999.
41. **Szpaderska AM, Walsh CG, Steinberg MJ, DiPietro LA.** Distinct patterns of angiogenesis in oral and skin wounds. *J Dent Res* 84: 309–314, 2005.
42. **Taketomi T, Yoshiga D, Taniguchi K, Kobayashi T, Nonami A, Kato R, Sasaki M, Sasaki A, Ishibashi H, Moriyama M, Nakamura K, Nishimura J, Yoshimura A.** Loss of mammalian Sprouty2 leads to enteric neuronal hyperplasia and esophageal achalasia. *Nat Neurosci* 8: 855–857, 2005.
43. **Taniguchi K, Sasaki K, Watari K, Yasukawa H, Imaizumi T, Ayada T, Okamoto F, Ishizaki T, Kato R, Kohno R, Kimura H, Sato Y, Ono M, Yonemitsu Y, Yoshimura A.** Suppression of Sproutys has a therapeutic effect for a mouse model of ischemia by enhancing angiogenesis. *PLoS One* 4: e5467, 2009.
44. **Wilgus TA, Ferreira AM, Oberyszyn TM, Bergdall VK, Dipietro LA.** Regulation of scar formation by vascular endothelial growth factor. *Lab Invest* 88: 579–590, 2008.
45. **Yigzaw Y, Cartin L, Pierre S, Scholich K, Patel TB.** The C terminus of sprouty is important for modulation of cellular migration and proliferation. *J Biol Chem* 276: 22742–22747, 2001.
46. **Zhang C, Chaturvedi D, Jaggar L, Magnuson D, Lee JM, Patel TB.** Regulation of vascular smooth muscle cell proliferation and migration by human sprouty 2. *Arterioscler Thromb Vasc Biol* 25: 533–538, 2005.